Spray Development for Low Temperature Combustion in an HSDI Optical Diesel Engine using Multiple Injection Strategies

Tiegang Fang*
Department of Mechanical and Aerospace Engineering
North Carolina State University
Raleigh, NC 27695-7910, USA

Robert E. Coverdill, Chia-fon Lee, and Robert A. White
Department of Mechanical Science and Engineering
University of Illinois at Urbana-Champaign
Urbana, IL 61801, USA

Abstract

In this paper, the spray development in an HSDI optical diesel engine was studied for low temperature combustion conditions by employing an advanced injection strategy with an early pre-TDC pilot injection followed by an after-TDC main injection. Heat release rates were calculated based on in-cylinder pressure. The spray development process for the entire cycle was visualized by using a high speed digital video camera synchronized with a high repetition rate copper vapor laser. Combustion process was also visualized by imaging the natural flame luminosity. From the experimental results, it is found that spray structure for the pilot injection is quite different from the main injection. Due to lower ambient pressure and temperature for early Pre-TDC injection timings, liquid spray shows highly dispersed structure with longer penetration. Depending on the pilot injection timing, fuel can penetrate into the squish region for earlier injection timings. Due to small fuel quantity, fuel impingement is rarely seen from the spray images. But for the main injection, much shorter liquid penetration is observed, which is resulted from the high pressure and high temperature ambiance with the piston close to the TDC. Due to the interaction of the spray jet with the piston bowl geometry, it is seen that fuel impingement occurs at the bowl lip, and this impingement splits the fuel spray into two parts with one going up into the squish region and the other going down into the piston bowl. This interesting observation was further confirmed by the combustion images with dual point ignition.

Introduction

Due to worldwide environmental concerns, the emission regulations have become more and more stringent. Exhaust emissions like oxides of nitrogen (NOx) and Particulate Matter (PM) must be reduced for diesel engines to meet future emission standards. Clean combustion technology should be developed to help solve these problems.

Multiple injection strategies have been reported for simultaneous reduction of NOx and PM in DI diesel engines [1-6]. Nehmer and Reitz [1] showed that pulsed injection might provide a method to reduce PM and allow for reduction of NOx from controlled pressure rise. The effectiveness of double, triple, and rate shaped injection strategies to simultaneously reduce NOx and PM was also evaluated [2]. Numerical simulations were used to study the mechanism of soot and NOx reduction for multiple injection strategies [3]. Zhang [4] investigated the effect of a pilot injection on NOx, soot emissions, and combustion noise in a small diesel engine. Simultaneous reduction of NOx and PM was obtained in an HSDI diesel engine by Chen [5]. Simultaneous reduction of combustion noise and emissions was possible through minimizing the fuel quantity and advancing the pilot injection timing [6].

Combustion concepts like Homogeneous Charge Compression Ignition (HCCI) combustion have been shown to be effective for NOx and PM reduction [7-10]. Due to the low volatility of diesel fuel, it is difficult to form a homogeneous charge for diesel engines. Because of the flexibility of the multiple injection strategies in controlling the mixing and combustion processes, they have been employed in DI diesel engines for HCCI-like combustion modes. Hashizume et al. [11] proposed a low soot solution, called MULtiple stage DIesel Combustion (MULDIC) for higher load operating conditions. A multi-pulse HCCI combustion study was done by Su et al.[12]. A study by Hasegawa and Yanagihara [13] employed two injections called UNIform BUlky combustion System (UNIBUS). A dual mode operation was used in a Narrow-Angle Direct-Injection (NADI^{TM}) concept [14]. The engine is operated in

*Corresponding author, Email: tfang2@ncsu.edu

HCCI combustion under partial loads and in conventional diesel combustion at full-load conditions. HCCI combustion in a small-bore HSDI diesel engine was investigated by using early multiple short injection pulses during the compression stroke [15]. Two-stage diesel fuel injection HCCI combustion was carried out by Kook and Bae [16]. A large fuel fraction was injected very early before TDC. A second injection with a small amount of fuel was injected near the compression TDC to ignite all the air-fuel mixtures. A study on smokeless rich combustion provided a wider range for low sooting and low NOx combustion [17]. By reducing temperature, the low sooting and low NOx combustion range can be expanded to rich mixture. Low temperature combustion with charge heterogeneity can be used to expand the low emission operating conditions to high-load regimes. Pickett [18] showed that mixing controlled diesel combustion was possible at lower flame temperatures with minimal NOx formation. Multiple injection strategies were applied in an optical HSDI diesel engine and results showed promising potential for implementing low temperature combustion with simultaneous reduction of soot and NOx [19, 20].

Liquid fuel distribution visualization in engine cylinder provides useful information on the evolution of diesel spray evaporation and fuel droplet dispersion. Mie-scattering technique is a commonly used method for liquid phase visualization [21-24]. Combustion visualization gives a qualitative feel for the effects of differing injection strategies. Imaging of the natural flame luminosity from the combustion event through the use of an optical engine has been a technique that has garnered widespread use [25-31]. These works identified ignition locations, flame temperatures, evidence of flame wall interaction and late cycle events such as soot oxidation.

This work is to study the spray development and combustion characteristics under low temperature combustion mode with a multiple injection strategy. The entire cycle spray and combustion events are visualized. The characteristics of sprays under early pilot injection timing and late main injection timing will be analyzed and discussed.

Table 1. Specifications of the single cylinder DIATA research engine conditions

Bore	70 mm
Stroke	78mm
Displacement/Cylinder	300 cc
Compression Ratio	19.5:1
Swirl Ratio	2.5
Valves/Cylinder	4
Intake Valve Diameter	24 mm
Exhaust Valve Diameter	21 mm
Maximum Valve Lift	7.30/ 7.67 mm (Intake/ Exhaust)
Intake Valve Opening	13 CAD ATDC (at 1 mm valve lift)
Intake Valve Closing	20 CAD ABDC (at 1 mm valve lift)
Exhaust Valve Opening	33 CAD BBDC (at 1 mm valve lift)
Exhaust Valve Closing	18 CAD BTDC (at 1 mm valve lift)

Optical Engine and Facility

A single-cylinder DIATA research engine supplied by Ford Motor Company was modified into the optical engine used for the current experimentation. Key aspects of the DIATA engine are listed in Table 1. The design is similar to the drop-liner design employed at Sandia National Labs in Livermore, CA. Optical access to the combustion chamber is attained from the side through a window just below the head, or from below through the fused silica piston top. The optical engine design maintains the geometry of the ports and combustion chamber of the original metal engine. A complete description of the optical engine and setup can be found in previous publications [19-20, 32-35]. A Bosch common-rail fuel injection system is used on the research engine, and is capable of rail pressures up to 1350 bar. The fuel injector used in this system is a valve-covered-orifice injector with six 0.124 mm holes placed symmetrically in the nozzle tip. The spray cone angle is 150 degrees. The injector is fitted with a needle lift sensor that allows the monitoring of the needle operation throughout injection. A Phantom v7.0 high-speed digital video camera was used to visualize the spray and combustion. A Copper-Vapor laser synched with the camera was used to illuminate the liquid fuel during the injection videos. National Instruments LabView version 6.0 was used as the data acquisition and timing software for the engine. An optical shaft encoder with 0.25 crank angle resolution was used to provide the time basis on which all data acquisition timing systems were operated. The engine temperatures and pressures were monitored through the use of a multifunction data acquisition board. The necessary timing involved in running the engine and cameras was performed through 16 32-bit counter/timers.

Engine Operating Conditions

The engine speed remained constant throughout experimentation at 1500 RPM. The injection pressure was 1000 bar. In each cycle, two injections were injected. Pilot injection fuel quantities of 0.8 mm^3 and 1.3 mm^3 were se-

lected. Pilot injection timings were set at –30 CAD ATDC and –40 CAD ATDC. The main injection timings were retarded to obtain low temperature combustion modes for these conditions. The main injection pulse duration was adjusted to match the load to be nominal 5.0 bar IMEP. Fuel used in these experiments was a low-sulfur European Diesel fuel. Due to the extensive optical access provided by the optical DIATA engine, 3-D like imaging was feasible [19-20, 33-35]. The high-speed video camera was operated by setting the resolution at 512X256 to capture the spray and combustion images from the side window and the bottom of the optical piston. The operating frame rate is 12000 frames per second. This frame rate corresponds to 0.75 CAD between two sequential images at 1500 rpm.

Table 2. Summary of engine operating conditions

Case Number	Rail Pressure [bar]	Pilot Timing [CAD ATDC]	Pilot Quantity [mm^3]	Main Timing [CAD ATDC]	IMEP [bar]
1	1000	-40	0.8	5	5.05
2	1000	-30	0.8	12	5.09
3	1000	-40	1.3	5	5.09
4	1000	-30	1.3	12	5.03

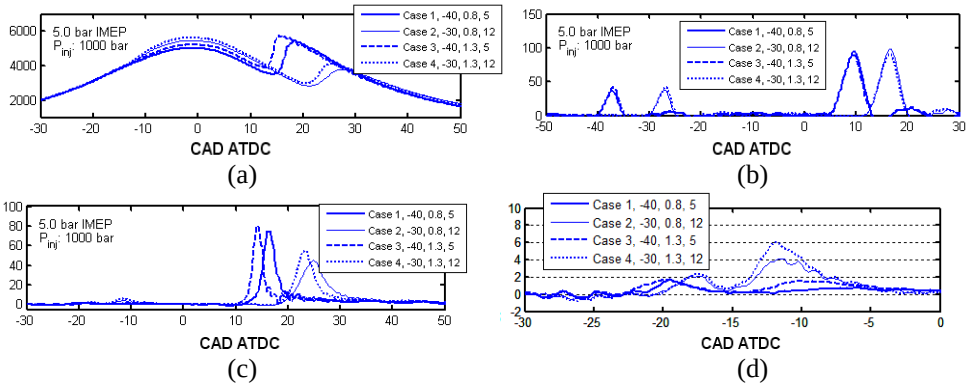

Figure 1 (a)The in-cylinder pressure in kPa; (b) needle-lift data in arbituary units; (c) heat release rate in J/deg; (d) amplified heat release rate for the pilot injection in J/deg.

Results and Discussion

IN-CYLINDER PRESSURE AND HEAT RELEASE ANALYSIS

The in-cylinder pressure, needle lift, and heat release rate for the 4 cases are shown in Figs. 1(a)-1(c). Ignition delay for the main injection is seen to be shorter for high pilot fuel quantity. Earlier pilot injection timing leads to lower TDC pressure before main injection due to incomplete combustion for earlier pilot injection timing with a too lean air-fuel mixture. Later main injection timing results in a soft combustion mode with lower pressure increasing rates. The needle lift data for these cases are shown in Fig. 1(b). Based on the needle lift, it is seen that higher pilot fuel quantity leads to a slightly longer injection duration. The main injection duration for Cases 1-4 is about 8.25 CAD and the difference among the four cases is less than 0.25 CAD. The heat release rate curves are shown in Fig. 1(c). Amplified heat release rate curves for the pilot injections are shown in Fig. 1(d) to clearly illustrate the heat release pattern. Similar to the observations in in-cylinder pressure data, higher pilot fuel quantity leads to shorter ignition delays. Because of later injection timing, the ignition delay is longer for the even-number cases than the odd number cases. A premixed-combustion-dominated heat release pattern is seen for all of the cases in the main injection. Retarded injection timing leads to wider heat release rate curves and lower heat release rate peak value.

For the pilot injection, although the heat release rate value is small, two-stage low temperature reaction pattern is seen for all of the 4 cases. Referring to the needle lift data for the pilot injection, the heat release starts later than the end of injection especially for earlier pilot injection timing cases. There is enough time for the fuel to mix with air. However, the heat release starting timing difference is less than the injection timing difference for the two pilot injection timings, which indicates that the low temperature combustion requires a certain ambient temperature to initiate the cool flame. Cool flame heat release occurs earlier for earlier pilot injection timing. However, the influence of fuel quantity on the cool flame occurring timing is rarely seen, showing that the overall equivalence ratio on the cool flame has relatively less effect than that of the ambient temperature [36]. Ambient temperature plays an important role in determining the start of cool flame. But higher pilot fuel quantity does lead to stronger two-stage

heat release. The dwell time between the cool flame and the second stage heat release is longer for earlier injection timing cases. The second-stage heat release is weaker for earlier pilot injection timing and lower fuel quantity, which leads to lower TDC in-cylinder temperature and pressure.

SPRAY DEVELOPMENT

The liquid spray developments of the pilot injection for Cases 1-4 are shown in Fig. 2. Due to the optical distortion of the optical piston, quantitative analysis is very difficult and only qualitative observations are presented in the paper. Fuel comes out of the nozzle hole at about 1.25~1.5 CAD ASOI. The injection is completed between 3.75~4.50 CAD ASOI. First spray image shows great asymmetry for the six jets. Later spray jets, however, are more symmetrical. The spray cone angle is wider for early injection timing cases, namely Cases 1 and 3, than later injection timing cases, say Cases 2 and 4. Longer spray penetration is seen for early injection timing cases. The reason for this might be due to a lower ambient air pressure and temperature. Lower ambient pressure and density make the spray tip penetrate further. At the same time, lower ambient temperature reduces the spray evaporation rate with longer spray development time. Another observation is that for earlier injection timing cases spray tips are seen in the squish region over the piston top. But for later first injection timing cases, no apparent liquid fuel is seen in squish region. Little spray impingement is seen for all the conditions. Slightly stronger Mie-scattering signal is seen for higher first fuel quantity cases near the end of injection.

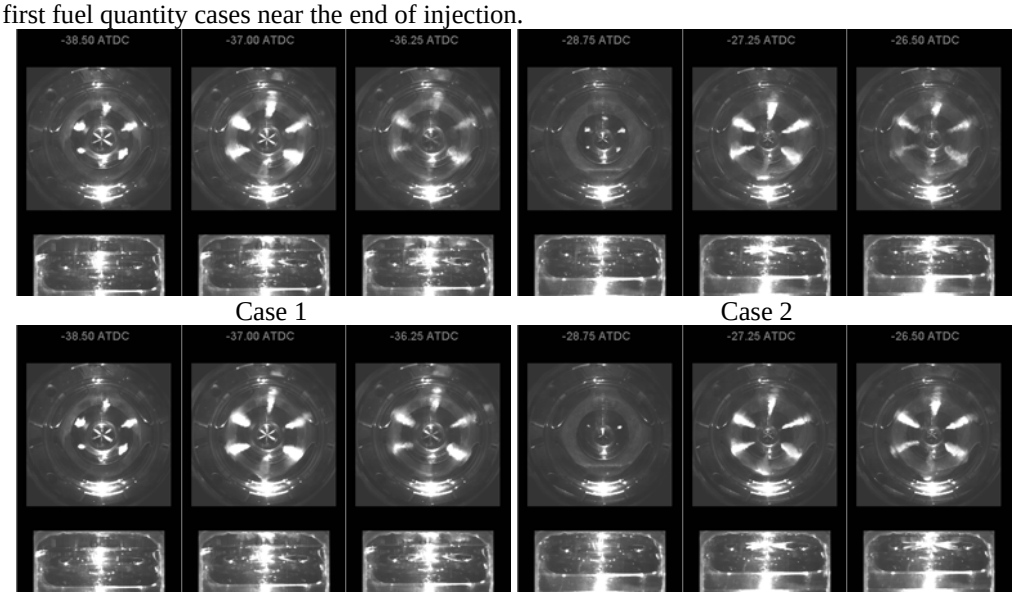

Figure 2 Mie-scattering spray images for the pilot injection of Cases 1-4

The second injection Mie-scattering images for the 4 cases are shown in Fig. 3. For Case 1, the fuel comes out of the nozzle hole between 0.75~1.5 CAD ASOI and injection completes at about 7.5 CAD ASOI. The six fuel jets are quite symmetrical for the whole injection event. Fuel impingement is seen on the bowl wall from the side window. From the bottom of the piston, the spray penetration is close to the maximum length and stays until the end of injection. At the end of fuel injection, no early combustion flame is observed for this case, which shows a highly premixed combustion occurs for Case 1. The spray development for Case 3 is quite similar to Case 1. But for Case 3, because higher first injection fuel quantity leads to a higher ambient temperature, the fuel penetration and wall impingement for Case 3 is seen slightly less than Case 1 as shown in the Mie-scattering images during the late injection stages. Another obvious difference is that early flame occurs earlier for Case 3 than Case 1 due to shorter ignition delay under higher ambient temperature. For Case 2, spray comes out of the nozzle hole at about 0.5~1.25 CAD ASOI and completes at about 7.25 CAD ATDC with very close injection duration to Case 1. Spray developments show similar observation to Case 1. Strong fuel impingement is seen for Case 2 with signal slightly higher than Case 1, which is due to later injection timing with less ambient density. Due to the later injection timing, the spray axis is more likely to intercept with the piston bowl lip. Some fuel goes into the squish region after impinging on the bowl lip as shown in the spray image at 17.00 CAD ATDC. This observation is more apparent when looking at the spray video. The fuel impingement on the bowl lip benefits the air-fuel mixing process and, consequently, a dual-region ignition pattern is found in the combustion flame under similar second injection timing. One ignition region is in the

bowl region near the bowl wall and the other is over the piston top in the squish region. This dual-region ignition results in a faster combustion process at the early stage. For Case 4, compared with Case 2, the injection duration is similar. Spray penetration and fuel impingement are seen shorter and weaker than Case 2 due to higher ambient temperature. The fuel impingement on the wall is obviously less different for Case 4 than Case 2.

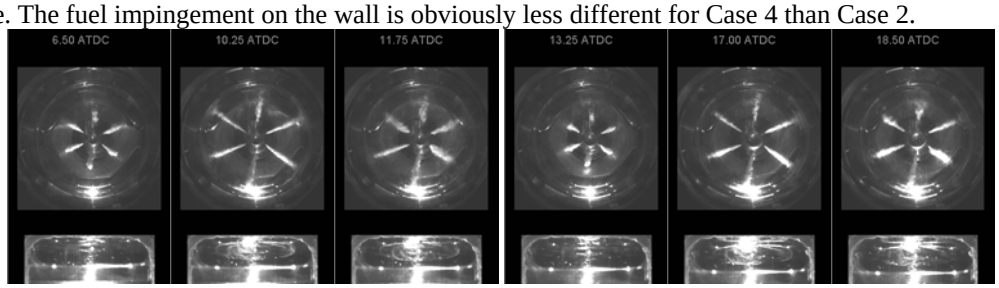

Case 1 Case 2

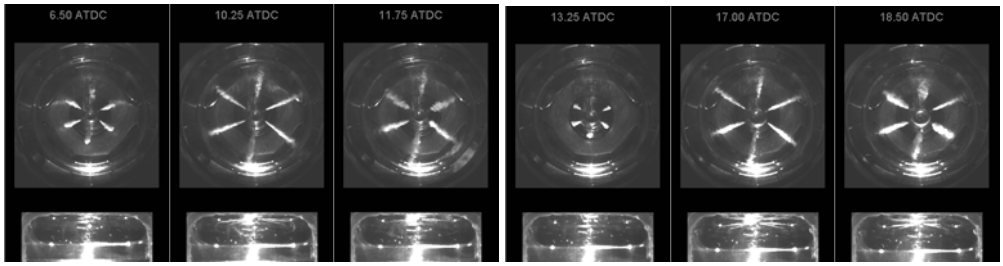

Case 3 Case 4

Figure 3 Mie-scattering spray images for the main injection of Cases 1-4

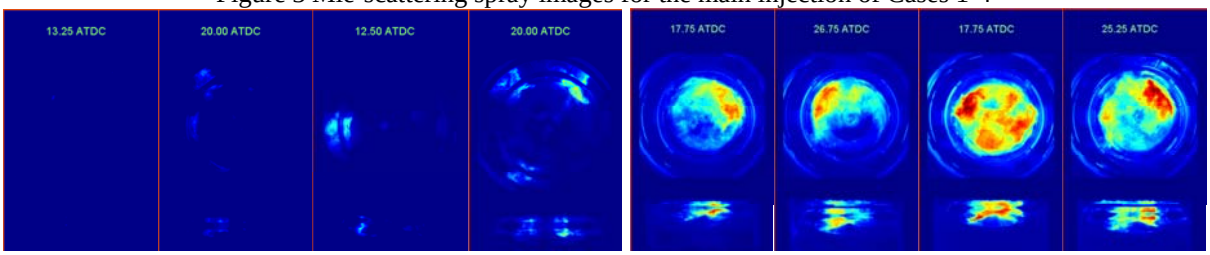

Case 1 Case 2 Case 3 Case 4 Case 1 Case 2 Case 3 Case 4

Figure 4 Combustion images for the 4 cases at two stages: early flame stage (left) and strong flame stage (right)

COMBUSTION IMAGES

The combustion images are shown in top row in Fig. 4 at a timing near the end of main injection. High luminosity indicates that there are more flame spray overlap indicating some liquid fuel is injected into early flames for some cases. An earlier pilot injection timing and small pilot fuel quantity have similar effects to high injection pressure. For Case 1, the early flame is so weak and it shows a typical premixed charge combustion mode. The early flame of Case 2 shows interesting observation with dual ignition locations, namely in the piston bowl (from the side window image) and in the squish region (from the bottom-viewed image). This can be explained by the fuel jet interaction with the bowl lip as discussed in the spray development section. A less spray and flame overlap time results in less fuel thermal cracking and less soot formation. Different from the conventional diesel combustion, the early flame combusts in a colder environment with less highly luminous flame for the low temperature combustion modes. The combustion images at the bottom show strong flame during the combustion process. At these crank angles, flame is mostly confined in the bowl region. Pilot injection timing and injection fuel quantity play minor roles in affecting the flame luminosity. Higher pilot fuel quantity leads to more luminous flame with more soot formation. The main injection timing also plays an important role in soot formation. Even though the pilot injection timing is earlier for the odd-number cases, the main injection timing is also earlier compared with the even-number cases. Therefore, a slightly stronger flame is found for the odd-number cases at these crank angles.

Conclusion

In this paper, the spray and combustion development in an HSDI optical diesel engine was studied for low temperature combustion conditions by employing an advanced injection strategy with an early pre-TDC pilot injection

followed by an after-TDC main injection. Heat release rates were calculated based on in-cylinder pressure. The spray development process for the entire cycle was visualized by using a high speed camera synchronized with a copper vapor laser. Combustion process was also visualized by imaging the natural flame luminosity. Spray structure for the pilot injection is quite different from the main injection. Due to lower ambient pressure and temperature for early Pre-TDC injection timings, liquid spray shows highly dispersed structure with longer penetration. Depending on the pilot injection timing, fuel can penetrate into the squish region for earlier injection timings. Due to small fuel quantity, fuel impingement is rarely seen from the spray images. But for the main injection, shorter liquid penetration is observed. Due to the interaction of the spray jet with the piston bowl geometry, fuel impingement occurs at the bowl lip for certain cases, and this impingement splits the spray into two parts with one going up into the squish region and the other going down into the piston bowl. This leads to a dual-point ignition process in the followed combustion event. This interesting observation of dual point ignition is further confirmed by the combustion images.

Acknowledgments

This work was supported in part by the Department of Energy Grant No. DE-FC26-05NT42634, by Department of Energy GATE Centers of Excellence Grant No. DE-FG26-05NT42622, and by the Ford Motor Company under University Research Program. We also thank Paul Miles of Sandia National Laboratories, Evangelos Karvounis and Werner Willems of Ford for their assistance on the design of the optical engine and on the setup of the experiments.

References

1. Nehmer, D.A. and Reitz, R.D. *SAE paper 940668*, 1994.
2. Tow, T.C., Pierpont, D.A. and Reitz, R.D. *SAE paper 940897*, 1994
3. Han, Z., Uludogan, A., Hampson, G.J. and Reitz, R.D. *SAE paper 960633*, 1996
4. Zhang, L. *SAE paper 1999-01-3493*, 1999
5. Chen, S.K. *SAE paper 2000-01-3084*, 2000
6. Tanaka, T., Ando, A. and Ishizaka, K. JSAE Review, 23: 297-302 (2002)
7. Onishi, S., Hong Jo, S., Shoda, K., Do Jo, P. and Kato, S. *SAE paper 790501*, 1979
8. Noguchi, M., Tanaka, Y., Tanaka, T. and Takeuchi, Y. *SAE paper 790840*, 1979
9. Najt, P.M. and Foster, D.E. *SAE paper 830264*, 1983
10. Thring, R.H. *SAE paper 892068*, 1989
11. Hashizume, T., Miyamoto, T., Akagawa, H. and Tsujimura, K. *SAE paper 980505*, 1998
12. Su, W., Lin, T. and Pei, Y. *SAE paper 2003-01-0741*, 2003
13. Hasegawa, R. and Yanagihara, H. *SAE paper 2003-01-0745*, 2003
14. Walter, B. and Gatellier, B. *SAE paper 2002-01-1744*, 2002
15. Helmantel, A. and Denbratt, I. *SAE paper 2004-01-0935*, 2004
16. Kook, S. and Bae, C. *SAE paper 2004-01-0938*, 2004
17. Akihama, K. et al., *SAE paper 2001-01-0655*, 2001
18. Pickett, L.M. *Proceedings of the Combustion Institute*, 30: 2727-2735 (2005)
19. Fang, T., Coverdill, R.E., Lee, C.F. and White, R.A. *SAE paper 2006-01-0078*, 2006
20. Fang, T., Coverdill, R.E., Lee, C.F., White, R.A. ICEF2007-1747, *ASME Fall Meeting*, Charleston, SC, 2007
21. Dec, J.E., Espey, C. *SAE paper 922307*, 1992
22. Honig, R., Kappler, G., Andresen, P., Brehm, N., *Combustion Sci. & Tech.* 102(1-6): 255-272 (1994)
23. Zhao, F.Q., Lai, M.C., Amer, A.A., Dressler, J.L., *Atomization and Sprays* 6(4): 461-483 (1996)
24. Becker, J., Hassa, C., *Atomization and Sprays*, 12(1-3): 49-67 (2002)
25. Miles, P. C., *SAE paper 2000-01-1829*, 2000
26. Arcoumanis, C., Cho, S. T., Gavaises, M. and Yi, H. S., *SAE paper 2000-01-1183*, 2000
27. Winterbourne, D. E., et al., *Proc. Instn. Mech. Engrs., Pt. C*, 208: 223-240 (1994)
28. Shiozaki, T., Nakajima, H., Yokota, H. and Miyashita, A., *SAE paper 980141*, 1998
29. Wang, T-C., Han, J-S., Xie, X., Lai, M-C. and Heinen, N. A., *SAE paper 1999-01-3496*, 1999
30. Bakenhus, M. and Reitz, R. D., *SAE paper 1999-01-1112*, 1999
31. Zambare, V. V. and Winterbourne, D. E., *SAE paper 1999-01-1501*, 1999
32. Mathews, W. S., Coverdill, R. E., Lee, C. F., and White, R. A., *SAE paper 2002-01-0266*, 2002
33. Fang, T., Coverdill, R.E., Lee, C.F. and White, R.A. *SAE paper 2005-01-0919*, 2005
34. Fang, T., Coverdill, R.E., Lee, C.F. and White, R.A. *SAE paper 2007-01-0203*, 2007
35. Fang, T., Coverdill, R.E., Lee, C.F. and White, R.A. *SAE paper 2008-01-1390*, 2008
36. Fang, T., Coverdill, R.E., Lee, C.F. and White, R.A. *SAE paper 2005-01-3838*, 2005